2017 IEEE Conference on Control Technology and Applications (CCTA)
August 27-30, 2017. Kohala Coast, Hawai'i, USA

Constraint Tightening for the Probabilistic Collision Avoidance of Multi-Vehicle Groups in Uncertain Traffic

Qian Wang[1], *Student Member, IEEE*, Beshah Ayalew[1], *Member IEEE*

***Abstract*— Future self-driving cars and current ones with advanced driver assistance systems are expected to interact with other traffic participants, which often are multiple other vehicles. To facilitate the motion planning of the autonomously controlled vehicle in collision avoidance, individual object vehicles with closeness in positions and velocities can be grouped as a single extended moving object. However, due to uncertainties from sensor imperfections and environmental disturbances, the collision avoidance conditions are often expressed as difficult to resolve probabilistic constraints in the motion planning problem. In this paper, we propose a constraint tightening method to transform the probabilistic collision avoidance condition for a vehicle group or an extended object into a deterministic form. This is done via a conservative closed-form transformation of the bivariate integral in the collision probability density function and subsequent computable approximation with logistic functions. Detailed numerical experiments are included to illustrate the workings and the performance of the proposed approach. This method can be incorporated in existing motion planning methods.**

I. INTRODUCTION

In the march towards (semi-)autonomous driving, the task of guiding the controlled vehicle in the presence of other traffic participants remains a challenging problem. Therein, tracking of moving objects plays a significant role. In particular, in public traffic, multiple other vehicles evolve in the traffic scene with changing velocity and position. From the perspective of guidance and control of the individual autonomously controlled vehicle (ACV), group tracking can facilitate safe motion planning decisions and control actions for the current and upcoming maneuvers of the ACV. Group tracking information can also constrain the nature of the interaction of the ACV and its subsequent motion like collision avoidance among the individual moving objects (primarily other vehicles in traffic).

In tracking of individual object vehicles from sets of measurements, e.g., sparse laser point cloud, each vehicle can be treated as an extended object with simple geometric shapes like a circle [1], an ellipse [2], rectangle [3] or some such arbitrary shape [4]. Data association approaches like Multi Hypothesis Tracking (MHT) [5], Probabilistic MHT (PMHT) [6], Probability Hypothesis Density (PHD) approach [7], Joint Probabilistic Data Association (JPDA) approach [8], or Random Finite Sets (RFS) [9] can be used to assign the measurements to each identified object vehicle. Therein, the object vehicles are represented by an estimated geometric/spatial shape (center and content parameters) and dynamics (position and velocity) [10].

The geometric shapes mentioned above are usually used in the motion planning problem to formulate the collision avoidance constraint. However, this problem is challenging for the following two principal reasons [11]: 1) the planning problem is non-convex as the feasible field is defined outside of the area occupied by the object vehicles, 2) the planning problem naturally involves uncertainties due to modeling error, sensor imperfections or environmental disturbances. To address these challenges, several approaches are proposed.

For the first challenge, polygonal models [11] [12], as a disjunction of linear constraints, or algebraic models like circles, ellipses [13] and hyper ellipses [14] are mostly used in the sampling-based planning method like RRT* algorithm [15]. However, for mathematical constrained-optimization based planning methods like MPC [16], algebraic models are better options than polygonal models because the disjunction of linear constraints will lead to discontinuity in the state space, which results in the Disjunctive Linear Programming problem [17]. This problem is similar as Mixed-Integer Programming problem that requires a specific solver to find a solution and is not efficient for real-time planning.

For the second challenge, the uncertainties can be handled by either considering their bounds (non-deterministic case) [18] or distribution (probabilistic case) [11] [19]. In the non-deterministic case, the worst case of the uncertainty is considered in the motion planning problem thus leading to a very conservative solution for the planning problem. However, in the probabilistic case, the computations are often intractable. However, for specified confident level/coefficient (e.g. probability of collision less than some small value), a solution can be obtained by solving an approximate deterministic motion planning problem with tightened constraints that account for the uncertainties. With assumptions of Gaussian distribution states, an efficient approximate explicit solution for probabilistic collision evaluation (in position description) was given in [19] for small-sized objects (radius smaller than 1 m). However, for a real normal-sized road vehicle, this approximation will not work. Thus, in our prior work [20], we developed a numerical method for evaluating the probability of closeness (including both position and forward velocity) between two individual object vehicles (IOVs) with non-negligible

1. Qian Wang and Beshah Ayalew are with the Applied Dynamics& Control Group at the Clemson University – International Center for Automotive Research (CU-ICAR), 4 Research Dr., 29607, Greenville, SC,USA, {qwang8, beshah}@clemson.edu

geometric shapes/sizes and used it for object grouping.

A given number of IOVs that have common movement (e.g. similar velocities) and geometrical proximity can be regarded as an object vehicle group (OVG) and represented as a single extended moving object. This helps to redefine the feasible collision-free field to exclude undesired local minimums (for the motion plan), as we illustrated in [21] with deterministic object motion models. Therein, we formed groups between detected object vehicles based on a distance threshold defined by the overlap of their elliptical collision fields. The identified vehicle groups are then represented with the tightest/optimal hyper-elliptical boundaries. Later in [22], we refined the object vehicle grouping method with a group structure evolution model and applied a supervised learning method to reduce the on-line computational efforts of generating the optimal (tightest) vehicle group boundaries. In [20], we extended the grouping method to the case with probabilistic uncertainties on the motion and measurement models. Therein, we proposed the probability of mutual closeness as criteria for vehicle group formation. This automatically considers closeness both in velocity and position in order for two objects to be in the same group. The collision boundary of the group is then defined as the joint position state distribution of those IOVs in the group with a specified confidence level or coefficient. However, the confidence level or coefficient is evaluated via a numerical integration method which is not efficient for real-time implementation.

The purpose of this paper is to develop an efficient computational method to tighten the probabilistic collision avoidance constraint in a deterministic way. Specifically, the contributions of this paper include:

- Derive a general integral form to evaluate the probabilistic collision avoidance constraint between an ACV and an IOV, both with non-negligible geometric shapes.
- Derive an explicit conservative transformation of the probabilistic collision avoidance constraint followed by a computable closed-form approximation
- Represent the multi-vehicle group (OVG) with an extended object vehicle and then tighten the probabilistic collision avoidance constraint between the ACV and the OVG using the above result.

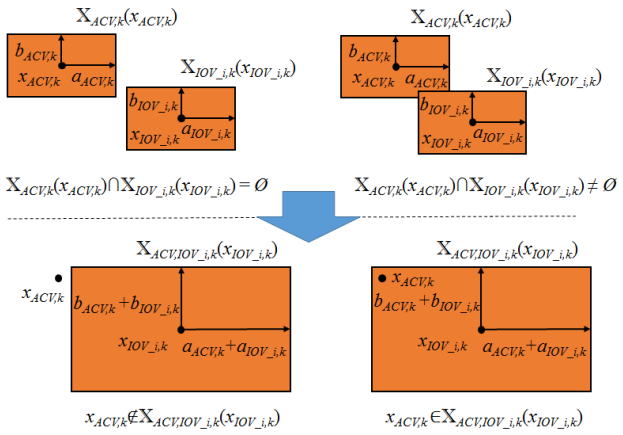

Figure 1 Example of the collision condition for ACV and IOV i with rectangular shape description in 2D (a is half length and b is half width)

The rest of the paper is organized as follows. Section II introduces the details the derivation of the probabilistic collision avoidance constraint as well the main steps for constraint tightening. Section III introduces the multi-vehicle grouping framework and the application of tightening the collision avoidance constraint. Section IV shows some illustrative numerical experiments. The potential application of the proposed method in motion planning of an autonomous vehicle is also illustrated in this section. Conclusions are included in Section IV.

II. Tightening the Probabilistic Collision Avoidance Constraint

A. Probabilistic Collision Avoidance Constraint

Considering the general discrete time evolution of the motion state and measurement sequence for a vehicle i:

$$x_{i,k} = f_{m,i}\left(x_{i,k-1}, w_{i,k-1}\right) \tag{1}$$

$$z_{i,k} = h_{m,i}\left(x_{i,k}, v_{i,k}\right) \tag{2}$$

where f_m is a (nonlinear) function of the state x and process noise sequence w. z is the available measurement. h_m is a (nonlinear) function of the states x and measurement noise sequence v.

In the Bayesian approach to tracking the motion of vehicle i, one attempts to estimate the posterior probability density function (PDF) $p_i(x_{i,k}|z_{i,1:k})$ of the states x_i according to all the measurements z_i up to time k. For a linear description of the motion and measurement system (1) and (2), the analytical solution for the exact posterior PDF can be obtained via the application of Kalman Filter (for Gaussian noise v and w,) and Grid-based Estimator (requiring discrete state space); For a nonlinear description of the system (1) and (2), Extended Kalman Filter or Unscented Kalman Filter, Approximate Grid-based Estimator and Particle Filter can be used to approximate the posterior PDF.

For collision identification for a specific time, without too much loss of generality, hereafter, x represents only the position state of the centroid of the geometric shape of each vehicle, for both the ACV and IOV. This because, unlike for grouping where both position and velocity closeness can be considered judging group formation, for physical collision identification only geometric closeness is relevant. Let $\mathbb{X}(x)$ be the geometric space (region or shape) occupied by a vehicle considering its geometric shape. Then, the collision between the ACV and IOV i at time k is defined by the condition $C(x_{ACV,k}, x_{IOV\_i,k})$: $\mathbb{X}_{ACV,k}(x_{ACV,k})\cap\mathbb{X}_{IOV\_i,k}(x_{IOV\_i,k})\neq\emptyset$, as shown in in Figure 1. Then, the probability that the ACV avoids collision with IOV i is higher than a specified confidence value $1-\delta$, $0<\delta<1$, can be given by:

$$P\left(X_{ACV,k}\left(x_{ACV,k}\right)\cap X_{IOV\_i,k}\left(x_{IOV\_i,k}\right)\neq\emptyset\right)\leq\delta \tag{3}$$

To simplify the evaluation of the collision probability we do some modification to the collision condition as well as the collision avoidance constraint as shown below:

$$P\left(x_{ACV,k} \in \mathbb{X}_{ACV,IOV\_i,k}\left(x_{IOV\_i,k}\right)\right) \le \delta \tag{4}$$

where $\mathbb{X}_{ACV,IOV\_i,k}(x_{IOV\_i,k})$ is an extended geometric space occupied by the IOV i at time k on which we lump the geometric shapes/sizes of the ACV $\mathbb{X}_{ACV,k}(x_{ACV,k})$ and IOV i $\mathbb{X}_{IOV\_i,k}(x_{IOV\_i,k})$. Therein, the ACV is considered as a point. Note that (3) and (4) are equivalent. An example of collision in 2D position space between ACV and IOV i with rectangular shapes is shown in Figure 1. One can also similarly derive the extended shape $\mathbb{X}_{ACV,IOV\_i}(x_{IOV\_i,k})$ for other geometric descriptions like circles or ellipses. However, rectangular shapes lead to closed-form solutions for the probability of collision.

As the state of the ACV and IOVs are estimated by the posterior PDF for the centroid of each vehicle, the probability of collision between the ACV and IOV i is defined by the integral of the joint position distribution of the ACV and IOV i:

$$P\left(x_{ACV,k} \in \mathbb{X}_{ACV,IOV\_i,k}\left(x_{IOV\_i,k}\right)\right) = \iint I_C\left(x_{ACV,k}, x_{IOV\_i,k}\right) p_{ACV,IOV\_i,k}\left(x_{ACV,k}, x_{IOV\_i,k}\right) dx_{ACV,k} dx_{IOV\_i,k} \tag{5}$$

where p_{ACV,IOV_i} is the joint position PDF of the ACV and IOV i, I_C is the collision indicator function defined by:

$$I_C\left(x_{ACV,k}, x_{IOV\_i,k}\right) = \begin{cases} 1, \text{ if } x_{ACV,k} \in \mathbb{X}_{ACV,IOV\_i,k}\left(x_{IOV\_i,k}\right) \\ 0, \text{ otherwise} \end{cases} \tag{6}$$

Using (6), (5) can be modified as:

$$P\left(x_{ACV,k} \in \mathbb{X}_{ACV,IOV\_i,k}\left(x_{IOV\_i,k}\right)\right) = \int \left[\int_{x_{ACV,k} \in \mathbb{X}_{ACV,IOV\_i,k}} p\left(x_{ACV,k} \mid x_{IOV\_i,k}\right) dx_{ACV,k} \right] p_{IOV\_i,k}\left(x_{IOV\_i,k}\right) dx_{IOV\_i,k} \tag{7}$$

As the inner integral of (7) constrains the range of $x_{ACV,k}$ within $\mathbb{X}_{ACV,IOV\_i,k}(x_{IOV\_i,k})$, we can define a deviation state variable $\Delta x_{IOV\_i,k} \in \mathbb{X}_{ACV,IOV\_i,k}(0)$ to replace $x_{ACV,k}$:

$$\int_{x_{ACV,k} \in \mathbb{X}_{ACV,IOV\_i,k}} p\left(x_{ACV,k} \mid x_{IOV\_i,k}\right) dx_{ACV,k} = \int_{\Delta x_{IOV\_i,k} \in \mathbb{X}_{ACV,IOV\_i,k}(0)} p\left(x_{ACV,k} = x_{IOV\_i,k} + \Delta x_{IOV\_i,k} \mid x_{IOV\_i,k}\right) d\Delta x_{IOV\_i,k} \tag{8}$$

where $\mathbb{X}_{ACV,IOV\_i,k}(0)$ is the lumped space when $x_{IOV\_i,k}$ is at the origin. Then,

$$P\left(x_{ACV,k} \in \mathbb{X}_{ACV,IOV\_i,k}\left(x_{IOV\_i,k}\right)\right) = \int \left[\int_{\Delta x_{IOV\_i,k} \in \mathbb{X}_{ACV,IOV\_i,k}(0)} p\left(x_{ACV,k} = x_{IOV\_i,k} + \Delta x_{IOV\_i,k} \mid x_{IOV\_i,k}\right) d\Delta x_{IOV\_i,k} \right] p_{IOV\_i,k}\left(x_{IOV\_i,k}\right) dx_{IOV\_i,k} \tag{9}$$

Assuming the distributions of the states of the ACV and IOV i are Gaussian and independent, (9) can be simplified further.

Proposition 1: Consider the ACV, with a point description with position state $x_{ACV,k}$ and IOV i, with an extended deterministic geometry description $\mathbb{X}_{ACV,IOV\_i,k}(x_{IOV\_i,k})$ with position state $x_{IOV\_i,k}$. If the states $x_{ACV,k}$ and $x_{IOV\_i,k}$ have Gaussian distributions, i. e., $x_{ACV,k} \sim N(m_{ACV,k}, \Sigma_{ACV,k})$, $x_{IOV\_i,k} \sim N(m_{IOV\_i,k}, \Sigma_{IOV\_i,k})$, and the state tracks of the ACV and IOV i are independent, then:

$$P\left(x_{ACV,k} \in \mathbb{X}_{ACV,IOV\_i,k}\left(x_{IOV\_i,k}\right)\right) = \int_{\Delta x_{IOV\_i,k} \in \mathbb{X}_{ACV,IOV\_i,k}\left(m_{ACV,k} - m_{IOV\_i,k}\right)} \frac{\exp\left[-\frac{1}{2} \Delta x_{IOV\_i,k}^T \left(\Sigma_{ACV,k} + \Sigma_{IOV\_i,k}\right)^{-1} \Delta x_{IOV\_i,k}\right]}{\sqrt{(2\pi)^{n_x} \left|\Sigma_{ACV,k} + \Sigma_{IOV\_i,k}\right|}} d\Delta x_{IOV\_i,k} \tag{10}$$

where n_x is the dimension of the position state x (n_x=2 for the 2D case). We have given the proof a similar statement as *Proposition 1* in [20]. Therefore, with (9) we have derived the general integral form for the probability of collision between the ACV and an IOV with non-negligible geometric shape and (10) gives the simplification for mutually independent motions with Gaussian uncertainty.

B. Constraint Tightening

To avoid the numerical evaluation of (10), in this paper, we seek to adopt an explicit formula that can approximate the integral so that the collision avoidance constraint can be evaluated rapidly for real-time applications. Considering the collision in a 2D case, the position state is defined by:

$$x = \begin{bmatrix} s \\ y_e \end{bmatrix} \tag{11}$$

where s and y_e are the arc length and lateral position for the centroid of the vehicle's geometric shape defined in the Frenet frame, as shown in Figure 2. $\kappa(s)$ is the curvature function of the reference path in terms of s. v^s is the velocity of the vehicle, the subscription t and n represent the tangential and normal direction with respect to the reference path. Here, we assume the forward direction of the vehicle's geometric shape is always consistent with its tangential velocity v_t^s.

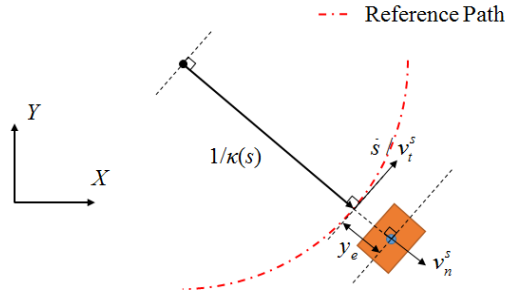

Figure 2. Motion description for the vehicle in the Frenet frame.

By following the assumptions used in *Proposition 1* and considering rectangular shapes for the vehicles, (10) can be rewritten as a definite bivariate normal integral:

$$P\left(x_{ACV,k} \in \mathrm{X}_{ACV,IOV\_i,k}\left(x_{IOV\_i,k}\right)\right) =$$
$$\int_{\Delta\underline{s}}^{\Delta\bar{s}}\int_{\Delta\underline{y}_e}^{\Delta\bar{y}_e} \frac{\exp\left[-\frac{1}{2}\left[\Delta s_{IOV\_i,k},\ \Delta y_{e,IOV\_i,k}\right]\Sigma^{-1}_{ACV,IOV\_i,k}\left[\Delta s_{IOV\_i,k},\ \Delta y_{e,IOV\_i,k}\right]^T\right]}{\sqrt{(2\pi)^{n_x}\left|\Sigma_{ACV,IOV\_i,k}\right|}} d\Delta s_{IOV\_i,k} d\Delta y_{e,IOV\_i,k} \tag{12}$$

where the integral region ($\Delta\underline{s}$, $\Delta\bar{s}$), ($\Delta\underline{y}_e$, $\Delta\bar{y}_e$) are defined by:

$$\begin{aligned}
\Delta\bar{s} &= \mathrm{m}_{s,ACV,k} - \mathrm{m}_{s,IOV_i,k} + a_{ACV,k} + a_{IOV_i,k} \\
\Delta\underline{s} &= \mathrm{m}_{s,ACV,k} - \mathrm{m}_{s,IOV_i,k} - a_{ACV,k} - a_{IOV_i,k} \\
\Delta\bar{y}_e &= \mathrm{m}_{ye,ACV,k} - \mathrm{m}_{ye,IOV_i,k} + b_{ACV,k} + b_{IOV_i,k} \\
\Delta\underline{y}_e &= \mathrm{m}_{ye,ACV,k} - \mathrm{m}_{ye,IOV_i,k} - b_{ACV,k} - b_{IOV_i,k}
\end{aligned} \tag{13}$$

and the combined covariance matrix $\Sigma_{ACV,IOV\_i,k}$ is given by:

$$\Sigma_{ACV,IOV\_i,k} = \begin{bmatrix} \sigma^2_{s,ACV,IOV\_i,k} & \rho\sigma_{s,ACV,IOV\_i,k}\sigma_{ye,ACV,IOV\_i,k} \\ \rho\sigma_{ye,ACV,IOV\_i,k}\sigma_{s,ACV,IOV\_i,k} & \sigma^2_{ye,ACV,IOV\_i,k} \end{bmatrix}$$
$$\sigma^2_{s,ACV,IOV\_i,k} = \sigma^2_{s,ACV,k} + \sigma^2_{s,IOV\_i,k}$$
$$\sigma^2_{ye,ACV,IOV\_i,k} = \sigma^2_{ye,ACV,k} + \sigma^2_{ye,IOV\_i,k} \tag{14}$$

where σ is the variance for each position state and ρ is the correlation coefficient between s and y_e. Without loss of generality, here we consider $|\rho|<1$. To efficiently and conservatively evaluate the probability of collision in (12) with $|\rho|<1$, we give the following closed-form approximation that voids the evaluation of the integral on the right-hand side of (12). We detail the derivations with general observations about bivariate normal distributions in *Remark 1* and *Remark 2*.

Remark 1: Let (X, Y) have a bivariate normal distribution with correlation coefficient ρ=0:

$$\begin{bmatrix} X \\ Y \end{bmatrix} \sim N\left(\begin{bmatrix} m_X \\ m_Y \end{bmatrix}, \begin{bmatrix} \sigma^2_X & 0 \\ 0 & \sigma^2_Y \end{bmatrix}\right) \tag{15}$$

The solution for the bivariate integral within the integral region ($\underline{X}$, $\bar{X}$), ($\underline{Y}$, $\bar{Y}$) is easy to obtain:

$$P\left(\underline{X} \le X \le \bar{X}, \underline{Y} \le Y \le \bar{Y}\right) =$$
$$\frac{1}{4}\mathrm{erf}\left(\frac{1}{\sqrt{2}\sigma_X}(X - m_X)\right)\Bigg|_{\underline{X}}^{\bar{X}} \mathrm{erf}\left(\frac{1}{\sqrt{2}\sigma_Y}(Y - m_Y)\right)\Bigg|_{\underline{Y}}^{\bar{Y}} \tag{16}$$

where erf is the error function:

$$\mathrm{erf}(x) = \frac{1}{\sqrt{\pi}}\int_{-x}^{x} e^{-t^2}\,\mathrm{d}t \tag{17}$$

This function can be approximated very-well by a logistic function [23]:

$$f_l(x) = \frac{2}{1+e^{-c_l x}} - 1 \tag{18}$$

with minimum cumulative square error found with the coefficient c_l=2.4, as illustrated in Figure 3. Therefore, (16) is rewritten by:

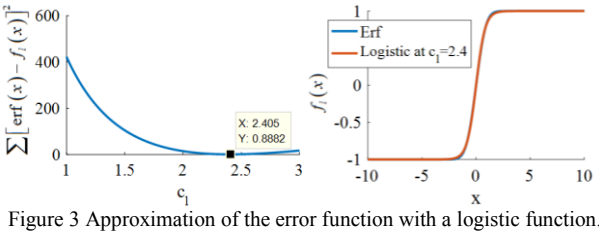

Figure 3 Approximation of the error function with a logistic function. The cumulative square error for 20000 samples range from -10 to 10 with different c_l values (Left). The approximation performance when c_l=2.4. The maximum error is 0.019 when |x| is close to 1.44 (Right).

$$P\left(\underline{X} \le X \le \bar{X}, \underline{Y} \le Y \le \bar{Y}\right) \approx$$
$$\frac{1}{4} f_l\left(\frac{1}{\sqrt{2}\sigma_X}(X - m_X)\right)\Bigg|_{\underline{X}}^{\bar{X}} f_l\left(\frac{1}{\sqrt{2}\sigma_Y}(Y - m_Y)\right)\Bigg|_{\underline{Y}}^{\bar{Y}} \tag{19}$$

Thus, we have arrived at a closed-form approximated solution for the cumulative probability of a bivariate normal distribution defined as (15).

Remark 2: Let (X, Y) have a bivariate normal distribution with zero means and correlation coefficient $|\rho|<1$:

$$\begin{bmatrix} X \\ Y \end{bmatrix} \sim N\left(\begin{bmatrix} 0 \\ 0 \end{bmatrix}, \begin{bmatrix} \sigma^2_X & \rho\sigma_X\sigma_Y \\ \rho\sigma_Y\sigma_X & \sigma^2_Y \end{bmatrix}\right) \tag{20}$$

It's hard to directly find the closed-form solution for the bivariate integral of this distribution, but it can be transformed into a bivariate normal distribution with ρ=0 (form of (15)) via a coordinate rotation, as shown in Figure 4. After rotation, the new distribution is given by:

$$\begin{bmatrix} X' \\ Y' \end{bmatrix} \sim N\left(\begin{bmatrix} 0 \\ 0 \end{bmatrix}, \begin{bmatrix} \sigma^2_{X'} & 0 \\ 0 & \sigma^2_{Y'} \end{bmatrix}\right) \tag{21}$$

The new self-variances $\sigma_{X'}$, $\sigma_{Y'}$ and the rotational 'angle θ can be determined by computing the eigenvalues and eigenvector of the old covariance matrix [24] to arrive at:

$$\sigma^2_{X'}, \sigma^2_{Y'} = \frac{\sigma^2_X}{2} + \frac{\sigma^2_Y}{2} \pm \frac{\sqrt{\sigma^4_X + 4\rho^2\sigma^2_X\sigma^2_Y - 2\sigma^2_X\sigma^2_Y + \sigma^4_Y}}{2} \tag{22}$$

$$\theta = -\arctan\left(\frac{\sigma^2_X}{2} + \frac{\sigma^2_Y}{2} - \frac{\sqrt{\sigma^4_X + 4\rho^2\sigma^2_X\sigma^2_Y - 2\sigma^2_X\sigma^2_Y + \sigma^4_Y}}{2\rho\sigma_X\sigma_Y} - \frac{\sigma_Y}{\rho\sigma_X}\right) \tag{23}$$

Note that different from the case in *Remark 1*, the X/Y

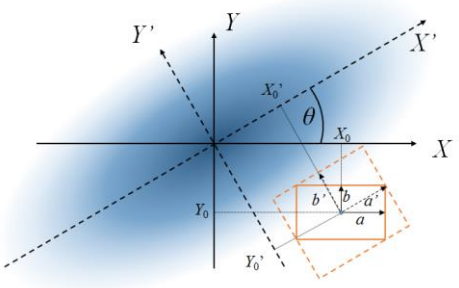

Figure 4 Bivariate normal distribution under different coordinate. $\rho\neq0$ in X/Y coordinate. ρ=0 in X'/Y' coordinate. The red rectangle represents the integral region.

coordinate and *X'/Y'* coordinate are both coordinates with their origins located at the means of the bivariate distribution (or are cases with zero means; non-zero mean distributions can be easily handled by applying translations with the means).

To apply the solution of the bivariate integral obtained from *Remark 1* to our problem, the rectangular integral region need to be rotated parallel with the axes of the new coordinate system. Also, to ensure a conservative evaluation of the probability, the new integral region must cover or circumscribe the old one. As shown in Figure 4, considering the original integral region $(\underline{X}, \overline{X}) = (X_0-a,\ X_0+a)$, $(\underline{Y}, \overline{Y}) = (Y_0-b,\ Y_0+b)$ in *X/Y* coordinate, we select the new integral region to be given by $(\underline{X}', \overline{X}') = (X_0'-a',\ X_0'+a')$, $(\underline{Y}', \overline{Y}') = (Y_0'-b', Y_0'+b')$ in *X'/Y'* coordinate, where:

$$\begin{bmatrix} X_0' \\ Y_0' \end{bmatrix} = \begin{bmatrix} \cos\theta & -\sin\theta \\ \sin\theta & \cos\theta \end{bmatrix} \begin{bmatrix} X_0 \\ Y_0 \end{bmatrix} \tag{24}$$

$$\begin{bmatrix} a' \\ b' \end{bmatrix} = \begin{bmatrix} \cos\theta & \sin\theta \\ \sin\theta & \cos\theta \end{bmatrix} \begin{bmatrix} a \\ b \end{bmatrix} \tag{25}$$

Then, a closed-form approximation of the cumulative probability of a bivariate normal distribution defined as (20) is conservatively obtained by:

$$P\left(\underline{X} \le X \le \overline{X}, \underline{Y} \le Y \le \overline{Y}\right) \le P\left(\underline{X}' \le X \le \overline{X}', \underline{Y}' \le Y \le \overline{Y}'\right) \approx \frac{1}{4} f_{\log}\left(\frac{1}{\sqrt{2}\sigma_{X'}} X'\right)\Bigg|_{\underline{X}'}^{\overline{X}'} f_{\log}\left(\frac{1}{\sqrt{2}\sigma_{Y'}} Y'\right)\Bigg|_{\underline{Y}'}^{\overline{Y}'} \tag{26}$$

Using this result, the probability of collision in (12) can be evaluated using the conservative integral region in the rotated coordinate system, which is then approximated in closed-form by the easy to evaluate logistic function.

III. Multiple Vehicle Grouping Framework

In [22], we proposed a probabilistic framework to track groups of IOVs. This framework follows a hierarchical estimation scheme to determine the group structure $\boldsymbol{G}$ from the state of all detected object vehicles at time *k*. The set, denoted by $\boldsymbol{X}$, of the states and geometrical shapes for all object vehicles is obtained by Bayesian IOV tracking with the measurement set $\boldsymbol{Z}$ from sensors. Then, a closeness matrix $\boldsymbol{M}_c$ between each pair of object vehicles is calculated via probabilistic collision checking considering uncertainties and geometrical shapes. The collision checking is used to evaluate the probabilistic collision between the IOVs, similar to condition (9), but considering the velocity state as well. Finally, a density-based clustering method (DBSCAN) with a specified probabilistic distance threshold ε is used to group/cluster the IOVs and determine the group structure state $\boldsymbol{G}$, which includes: 1) x_G, the estimated states (of a representative point, e.g. centroid) of the group as well as their covariance, 2) S_G, a parameters set (or generally, an algebraic function) that is used to describe the current shape/contour of the group when considered as an extended rigid object, and 3) I_G, the index set of the IOVs that belongs to the group, and 4) B_G, the OVG behavior indicating the group structure change from the last time step. Details can be found in [22].

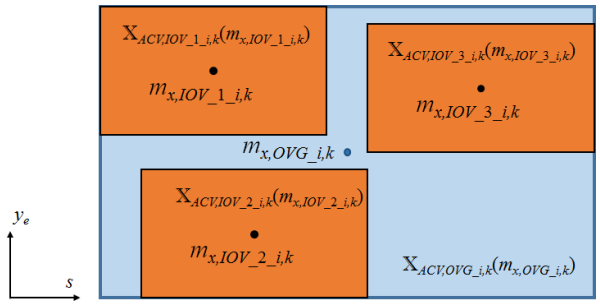

Figure 5 Illustration of the extended geometric shape for the OVG *i*

From the probabilistic grouping results, the probability of avoiding a collision with a certain OVG *i* can be described by the joint probability of collision avoidance with all the IOVs in the OVG *i*. Specifically, with a confidence value 1-δ, $0<\delta<1$, of the ACV to avoid collision avoidance with OVG *i* at time *k*, the constraint is given by:

$$P\left(\bigcup_{j\in I_{G,i,k}} x_{ACV,k} \in \mathbb{X}_{ACV,IOV\_j,k}\left(x_{IOV\_j,k}\right)\right) \le \delta \tag{27}$$

Applying Boole's inequality [25], (27) can be conservatively converted to:

$$\sum_{j=1}^{N_{I_{G,i,k}}} P\left(x_{ACV,k} \in \mathbb{X}_{ACV,IOV\_j,k}\left(x_{IOV\_j,k}\right)\right) \le \delta \tag{28}$$

where $N_{IG,i,k}$ is the number of the IOVs in OVG *i*. We can see that using (28), evaluating the constraint for ACV to avoid a collision with OVG *i* could be computationally expensive when $N_{IG,i,k}$ is large number. This will deteriorate the performance of real-time motion planning method like MPC or RRT* that requires high frequency update of the solution plan for avoiding collision. To overcome this issue, here we consider the OVGs as an individual extended object. The idea comes from our previous work [21] [22]. The extended shape can be obtained from the union of the geometric shapes of all the IOVs in the group. An example for a rectangular shape description is shown in Figure 5. The collision avoidance condition is thus transformed to avoiding collision with an extended object formed by the group. Therefore, (28) becomes:

$$P\left(x_{ACV,k} \in \mathbb{X}_{ACV,OVG\_i,k}\left(x_{OVG\_i,k}\right)\right) \le \delta \tag{29}$$

with Gaussian uncertainty assumption, (12) or the approximation (26) can be used to evaluate (29) with the integral regions defined by:

$$\begin{aligned} \Delta\overline{s} &= \mathrm{m}_{s,OVG\_i,k} + a_{ACV,OVG\_i,k} \\ \Delta\underline{s} &= \mathrm{m}_{s,OVG\_i,k} - a_{ACV,OVG\_i,k} \\ \Delta\overline{y}_e &= \mathrm{m}_{ye,OVG\_i,k} + b_{ACV,OVG\_i,k} \\ \Delta\underline{y}_e &= \mathrm{m}_{ye,OVG\_i,k} - b_{ACV,OVG\_i,k} \end{aligned} \tag{30}$$

where

$$\mathrm{m}_{s,OVG\_i,k} = \frac{\max\left(\mathrm{m}_{s,IOV\_I_{G,i},k} + a_{ACV,IOV\_I_{G,i},k}\right) + \min\left(\mathrm{m}_{s,IOV\_I_{G,i},k} - a_{ACV,IOV\_I_{G,i},k}\right)}{2}$$

$$\mathrm{m}_{ye,OVG\_i,k} = \frac{\max\left(\mathrm{m}_{ye,IOV\_I_{G,i},k} + b_{ACV,IOV\_I_{G,i},k}\right) + \min\left(\mathrm{m}_{ye,IOV\_I_{G,i},k} - b_{ACV,IOV\_I_{G,i},k}\right)}{2}$$

$$a_{ACV,OVG\_i,k} = \max\left(\mathrm{m}_{s,IOV\_I_{G,i},k} + a_{ACV,IOV\_I_{G,i},k}\right) - \mathrm{m}_{s,OVG\_i,k}$$

$$b_{ACV,OVG\_i,k} = \max\left(\mathrm{m}_{ye,IOV\_I_{G,i},k} + b_{ACV,IOV\_I_{G,i},k}\right) - \mathrm{m}_{ye,OVG\_i,k} \tag{31}$$

From (30), (31), as the extended geometric shape of OVG *i* covers more area than the union of the IOVs in the group, it will sacrifice some feasible regions for collision free plans. However, it helps to exclude some local minima and reduce the time to evaluate the collision constraint for the planning problem. We will demonstrate this via simulation in the next session.

According to (28), we can see the IOVs that are closer to the ACV in the OVG *i* will have more influence on the accumulative collision probability. In addition, accounting for the uncertainties on the position state of the ACV, the combined covariance matrix $\Sigma_{ACV,OVG\_i,k}$ between the ACV and OVG *i* can be selected from the set of the combined covariance matrix $\Sigma_{ACV,IOV\_I_{G,i},k}$ between the ACV and the IOVs in OVG *i*:

$$\Sigma_{ACV,OVG\_i,k} = \Sigma_{ACV,IOV\_j_{MD\min,G,i},k} \tag{32}$$

where $j_{MD\min,G,i}$ is the index for the IOV in OVG *i* with the minimum Euclidean distance to the ACV:

$$MD_{\min,G,i,k} = \min_{j \in I_{G,i,k}} \left(\sqrt{\left(s_{ACV,k} - s_{IOV\_j,k}\right) + \left(y_{e,ACV,k} - y_{e,IOV\_j,k}\right)}\right) \tag{33}$$

Therefore, by determining the size, the estimated position and the covariance matrix for the extended geometric shape of OVG *i,* the avoidance condition (29) can be evaluated.

IV. Results and Discussion

To illustrate the performance of the proposed constraint tightening method, we include the setup and results of some simulation comparisons for the boundary of the probabilistic collision of the ACV with: Case 1) a single IOV to compare the tightened constraint with different confidence values under numerical integration of the integral in (12) and the approximation of integral in (26); Case 2) an OVG with 3 IOVs inside it with fixed-group structure to compare the tightened group constraint with numerical integration via (28) and (29); and Case 3) an OVG with a dynamic group structure to compare the tightened constraint under numerical integration combining (12) and (28) to the approximation method via (26) and (29). The simulation is executed on an Intel Dual Core i5-4200M 2.4 GHz processor and 4GB RAM.

Figure 6 shows the probabilistic collision avoidance constraint tightening for Case 1: ACV with a single IOV. We compare the contour of the tightened constraint with different confidence values under numerical integration of the integral in (12) (referred too here as "actual") and the approximation method in (26). We can see at ρ=0, the actual constraint and the approximation are the same. As $|\rho|$ rises, the approximation error increases, but the approximation is always more conservative than the actual constraint. The conservatism is due to the additional integral region generated by (24), (25). Also, by using a closed-from approximation, the average time t_a to evaluate the constraint for a pair of estimated ACV and IOV positions is more than 40x faster than the numerical integration.

Figure 7 shows the probabilistic collision avoidance constraint tightening for Case 2: ACV with OVG with fixed group structure. We compare the case with actual constraint evaluation via (28) and the approximated constraint evaluation via (29). We can see the approximation case will generate a conservative rectangular area that covers all the probabilistic collision area between the ACV and IOVs. This keeps the number of evaluations of the probabilistic collision avoidance constraint equal to one per OVG. Therefore, the average computing time will not rise with the number of IOVs in the OVG as (28). Also, it excludes the local minimum generated by the union of avoiding collision with individual IOVs and the lane boundary, as shown in the area marked by red ellipse. When combined with the approximation of bivariate integral in (26), a more conservative and faster performance will be obtained, as shown in the next case.

The probabilistic collision avoidance constraint tightening for Case 3: ACV with OVG with dynamic

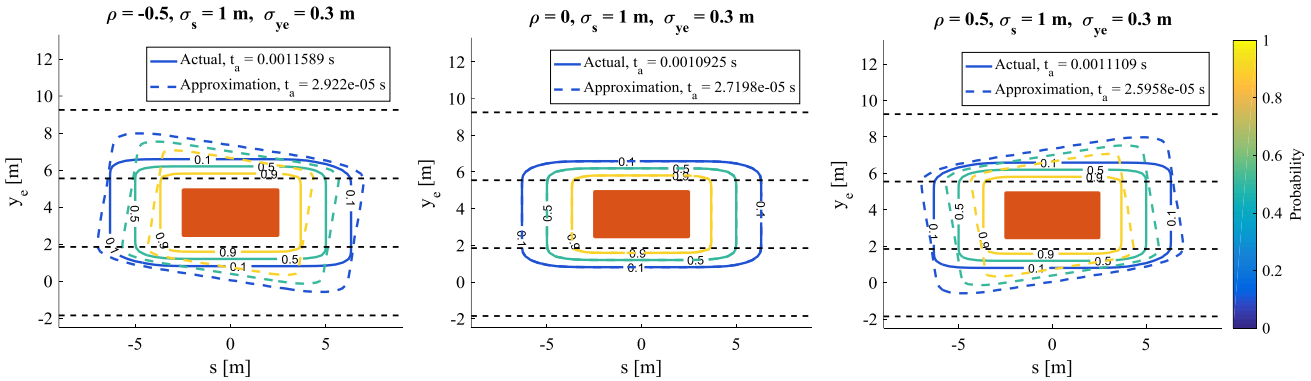

Figure 6 Illustration of the collision avoidance constraint tightening for a single IOV case with different correlation coefficient ρ. σ is the combined state variance including both ACV and IOV effect in (14). Actual and approximation case are evaluated by (12) and (26), respectively.

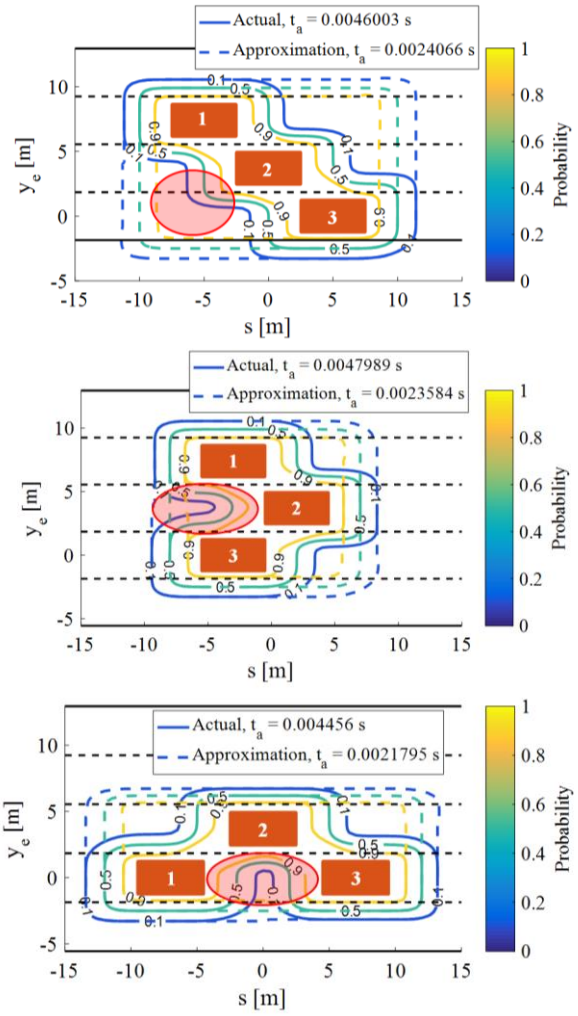

Figure 7 Illustration of the collision avoidance constraint tightening for an OVG case with different uncertainties: ρ_1=0.5, $\sigma_{s,1}$=1.1, $\sigma_{ye,1}$=0.6; ρ_2=0, $\sigma_{s,2}$=1, $\sigma_{ye,2}$=0.4; ρ_3=-0.3, $\sigma_{s,3}$=0.9, $\sigma_{ye,3}$=0.5. σ is the combined state variance including both the ACV and IOV in (14). Actual and approximation cases are evaluated by (28) and (29), respectively.

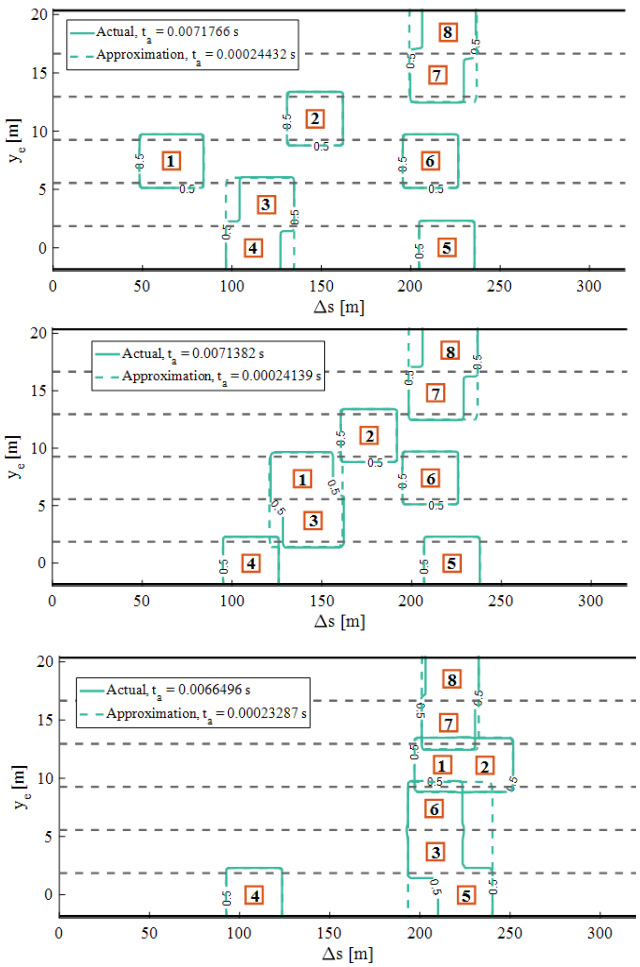

Figure 8 Illustration of the collision avoidance constraint tightening (only the contours with confidence value equal to 0.5 are shown) for an OVG case with dynamic group structure. The figures are sampled from a dynamic profile at time instance 0, 15 and 45s (from top to bottom). Actual case is evaluated by (12) and (28) while the approximation case is evaluated by (26) and (29).

structure is illustrated via three sampling instances (t=0s, 15s and 45s) in an evolving traffic shown in Figure 7. We compare the case with actual constraint evaluation (via (12) and (28)) and the approximated constraint evaluation (via (26) and (29)). In the simulation setting, IOV 1 intends to be driving around 30m/s, IOV 2 keeps constant velocity around 27m/s, and IOV 3 intends to pass IOV4 and then catch up with IOV 5 and IOV6. The rest of the IOVs are going round 25m/s. All the motions of IOVs are estimated by Kalman filter with position measurements, and the grouping is done by clustering with thresholded collision probabilities as described earlier and in [20]. Then, the method proposed in this paper is used to evaluate the probability of avoiding collision with those IOVs and OVGs at different instances. We can see the proposed method generates more conservative collision avoidance constraints for all cases. Also, the average time to evaluate the constraint with approximation method is much faster than the actual (numerical integration). The more number of OVGs are identified the faster the approximation method will be relative to individual evaluations, as the total number of constraint evaluation between the ACV and (extended) IOVs reduces (6 for the case at t=0s and 15s, but 4 for the case at t=45s).

From the simulation results above, we can see the approximation method can quickly and conservatively evaluate the probability of collision avoidance of an ACV with both IOVs and OVGs. In other words, once the uncertainty propagation of the ACV and IOVs in a short future horizon are predicted, the tightened collision avoidance constraint with specified confidence values can be easily determined. Therefore, this result has a potential use in the real-time motion planning of autonomous vehicles in uncertain public traffic involving many vehicles. Such planning frameworks were discussed, for example, our previous work [16] that discusses predictive control approaches and even those of [15] that use rapidly exploring random trees.

V. Conclusion

In this paper, we first derived a general integral form for evaluating the probabilistic collision avoidance condition

between an autonomously controlled vehicle (ACV) and an IOV, where both of which have non-negligible geometric shape information. Then, we outline a computationally efficient method is to evaluate the probabilistic collision avoidance constraint in a deterministic way. This is achieved by getting around the evaluation of the bivariate integral of the collision avoidance condition via exact coordinate transformations on the probabilistic condition followed by a function approximation. We show empirically and intuitively that this function approximation can be controlled so that the overall computation is conservative, i.e., it can be applied to tighten the probabilistic collision avoidance constraint. Furthermore, we show by extension that the result can be adopted to evaluate the collision avoidance condition between the ACV and the OVG where the latter is considered as extended geometric shape and locally computed covariance. The performance of the proposed constraint tightening method is illustrated via numerical experiments involving an ACV and other individual vehicles and some with fixed and dynamic group structures. In continuing work, we will apply the tightened collision avoidance constraint in the real-time stochastic motion planning algorithms for autonomous vehicles.

VI. REFERENCES

[1] N. Petrov, L. Mihaylova, A. Gning and D. Angelova, "A novel sequential Monte Carlo approach for extended object tracking based on border parameterisation," in *In Information Fusion (FUSION), 2011 IEEE Proceedings of the 14th International Conference on*, 2011.

[2] B. Ristic and D. Salmond, "A study of a nonlinear filtering problem for tracking an extended target," in *2004 IEEE Seventh International Conference on Information Fusion*, 2004.

[3] K. Granstrom and M. Baum, "Extended object tracking: introduction, overview and applications," 2016. [Online]. Available: https://arxiv.org/abs/1604.00970.

[4] M. Baum and U. D. Hanebeck., "Shape tracking of extended objects and group targets with star-convex RHMs," in *Information Fusion (FUSION), 2011 IEEE Proceedings of the 14th International Conference on*, 2011.

[5] D. Reid, "An algorithm for tracking multiple targets," *IEEE transactions on Automatic Control,* vol. 24, no. 6, pp. 843-854, 1976.

[6] P. Willett, Y. Ruan and R. Streit, "PMHT: problems and some solutions," *IEEE Transactions on Aerospace and Electronic Systems,* vol. 38, no. 3, pp. 738-754, 2002.

[7] B. Vo and W. Ma, "The Gaussian mixture probability hypothesis density filter," *IEEE Transactions on signal processing,* vol. 54, no. 11, pp. 4091-4104, 2006.

[8] Y. Bar-Shalom and E. Tse, "Tracking in a cluttered environment with probabilistic data association," *Automatica,* vol. 11, no. 5, p. 451–460, 1975.

[9] B.-N. Vo, S. Singh and A. Doucet, "Sequential Monte Carlo methods for multitarget filtering with random finite sets," *IEEE Transactions on Aerospace and electronic systems,* vol. 41, no. 4, pp. 1224-1245, 2005.

[10] S. Wender and K. Dietmayer, "3D vehicle detection using a laser scanner and a video camera," *IET Intelligent Transport Systems,* vol. 2, no. 2, pp. 105-112, 2008.

[11] L. Blackmore, H. Li and B. Williams, " A probabilistic approach to optimal robust path planning with obstacles," in *American Control Conference*, 2006.

[12] J. Nilsson, P. Falcone, M. Ali and J. Sjöberg, "Receding horizon maneuver generation for automated highway driving," *Control Engineering Practice,* vol. 41, pp. 124-133, 2015.

[13] U. Rosolia, F. Braghin, A. Alleyne and E. Sabbioni, "NLMPC for Real Time Path Following and Collision Avoidance," *SAE International Journal of Passenger Cars-Electronic and Electrical Systems,* vol. 8, no. 2, pp. 401-405, 2015.

[14] M. S. Menon and A. Ghosal, "Obstacle avoidance for hyper-redundant snake robots and one dimensional flexible bodies using optimization," in *14th World Congress in Mechanism and Machine Science*, Taipei, Taiwan, 2015.

[15] Y. Kuwata, J. Teo, G. Fiore, S. Karaman, E. Frazzoli and J. P. How, "Real-time motion planning with applications to autonomous urban driving," *IEEE Transactions on Control Systems Technology,* vol. 17, no. 5, pp. 1105-1118, 2009.

[16] Q. Wang. B. Ayalew. Thomas Weiskircher, "Predictive Guidance and Control Framework for (Semi-)Autonomous Vehicles in Public Traffic," *IEEE Transactions on Control Systems Technology ,* vol. PP, no. 99, pp. 1-13, 2017.

[17] E. Balas, "Disjunctive programming," *Annals of Discrete Math,* vol. 5, pp. 3-51, 1979.

[18] Y. Kuwata, T. Schouwenaars, A. Richards and J. How, "Robust constrained receding horizon control for trajectory planning," in *AIAA Guidance, Navigation, and Control Conference and Exhibit*, 2005.

[19] N. E. Du Toit and J. W. Burdick, "Probabilistic collision checking with chance constraints," *IEEE Transactions on Robotics,* vol. 27, no. 4, pp. 809-815, 2011.

[20] Q. Wang and B. Ayalew, "A Probabilistic Framework for Tracking the Formation and Evolution of Multi-Vehicle Groups in Uncertain Traffic," *IEEE Transactions on Intelligent Transportation Systems (Submitted, in review),* 2017.

[21] Q. Wang and B. Ayalew, "Obstacle Filtering Algorithm for Control of an Autonomous Road Vehicle in Public Highway Traffic," in *Proceedings of the ASME 2016 Dynamic System and Control Conference (DSCC)*, Minneapolis, MN., 2016.

[22] Q. Wang and B. Ayalew, "A multiple vehicle group modelling and computation framework for guidance of an autonomous road vehicle," in *Proccedings of the 2017 American Control Conference (Submitted)*, 2017.

[23] S. R. Bowling, M. T. Khasawneh, S. Kaewkuekool and B. R. Cho, "A logistic approximation to the cumulative normal distribution," *Journal of Industrial Engineering and Management,* vol. 2, no. 1, pp. 114-127, 2009.

[24] D. C. A. C. Constable, "Chapter 4: Multivariate Distributions. in Geophysical Data Analysis: Statistics," 2008. [Online]. Available: http://igppweb.ucsd.edu/~agnew/Courses/Sio223a/sio223a.chap4.pdf. [Accessed 9 3 2017].

[25] A. F. Karr, Probability, New York: Springer-Verlag, 1993.